مجلة التربوي

مجلة علمية محكمة تصدر عن كلية التربية

جامعة المرقب

العدد الثالث عشر
يوليو 2018م

هيئـــــــة التحريـــر

بحوث العدد

- Vocabulary knowledge and English reading obstacles faced by Libyan Undergraduate students at Elmergib University
- Difficulties Encountered by some Libyan Third – Year Secondary School Students in Forming and Using English Future Tenses
- An Acoustic Study of Voice On Investigating the difference between the effects of inductive and deductive approach in teaching grammar for sixth grade students in Anahda primary School
- Using Data Mining techniques in tracking the students' behavior in the asynchronous e-learning systems

G. E. A. Muftah[a] , A.M. Alshuaib[a] , E. M. Ashmila[b]

[a]Faculty of Science, University of bani walid, Bani Walid, Libya.

[b] Faculty of Education, University of Elmergib, Al-Khums, Libya

Abstract

Copper indium ditelluride ($CuInTe_2$) has been electrochemically deposited from aqueous solution. Cyclic voltammetry analyses were used to determine suitable deposition parameters. pH-potential diagram was drawn to provide information on the chemical reactions taking place at different deposition potentials and pH. As measured by Talysurf and gravimetric techniques, the thickness of deposited films was found to be ~2.0 μm, when deposited over a period of 3 hrs. X-ray diffraction, and optical absorption have been used to investigate the bulk structure, energy band gap of the material layers respectively. It was found that it has polycrystalline chalcopyrite structure with band gap varied between 1.10 and 1.30 eV.

Keywords: Electrodeposition of semiconductors, $CuInTe_2$, Thin film solar cells.

1- Introduction

One of the most promising materials for fabrication of low-cost thin film solar cells are the ternary I-III-VI_2 semiconductors having a chalcopyrite structure. The most studied member of this family is $Cu(In,Ga)Se_2$, which has a direct band gap (~1.20 eV) and a high absorption coefficient (~10^5 cm^{-1}). Interest in these materials increased since an also an efficiency of 12.8% has been achieved [1] and even of 19.9% was reported by the NREL group [2]. However, the efficiency of $Cu(In,Ga)Se_2$ seems to be saturated, and further improvements require deeper understanding of the underlying physics of the device, in addition to the optimization of material growth and the post-deposition processing steps. The high volatility of selenium is an important challenge in producing this material, which can be alleviated by substituting it with tellurium. This paper represents the growth of $CuInTe_2$ using a low-cost electro-deposition technique, characterizing its structure, absorption and bandgap. Some of electro-deposition techniques' advantages are; the low cost requirement, capability for large area growth, and the use of normal laboratory conditions for growing materials without the requirement of vacuum systems [3].

2- Experimental aspects

The $CuInTe_2$ layers were electrodeposited at room temperature (RT) on glass/FTO substrates from a solution containing 1 mM $CuCl_2$, 10 mM $InCl_3$ and 2 mM TeO_2, plus 0.5 M citric acid. The citric acid was used to dissolve TeO_2 in the aqueous solution. All chemicals had 5N purity, and the pH of the as-prepared solution was 1.57. A high purity carbon plate was used as the anode, and Ag/AgCl (+0.222 V versus NHE at RT) electrode was used as the reference electrode for the electro-deposition of $CuInTe_2$ in a three-electrode deposition system. Deposition was carried out under potentiostatic conditions using a fully automated Gillac potentiostat. The results discussed in this report are for room temperature and an unstirred system which produces layers with better adhesion and more uniform properties.

Prior to electro-deposition, the glass/FTO substrates were degreased in acetone and cleaned in deionized milli-Q water followed by a 2-min ultrasonication.

The $CuInTe_2$ layers were annealed at 400°C for 20 minutes in air and characterized using XRD (Phillips-1710) for structural properties, Tallysurf (Taylor-Hobson Tallysurf 1204L) for film thickness, and optical absorption (UNICAM UV/Visible Spectrometer) for the energy band gap.

1. pH-potential diagram of $CuInTe_2$

In order to establish suitable conditions for the electro-deposition of $CuInTe_2$ from a bath containing Cu_2^+, In^{+3}, $HTeO_2^+$ at R.T, pH-potential diagram was drawn to provide information on the chemical reactions taking place at different deposition potentials and pH. The Nernst equation was used to build up the diagram. Since there is no available thermodynamic data for the Cu-In-Te-H_2O system; the potential-pH diagram for this system could not be established. Therefore, the diagrams for both Cu-Te-H_2O, Figure 1(a) and In-Te-H_2O, Figure 1(b) systems were drawn and overlapped. The overlapped diagrams were used to establish the best region to grow the material as presented in Figure 1(c).

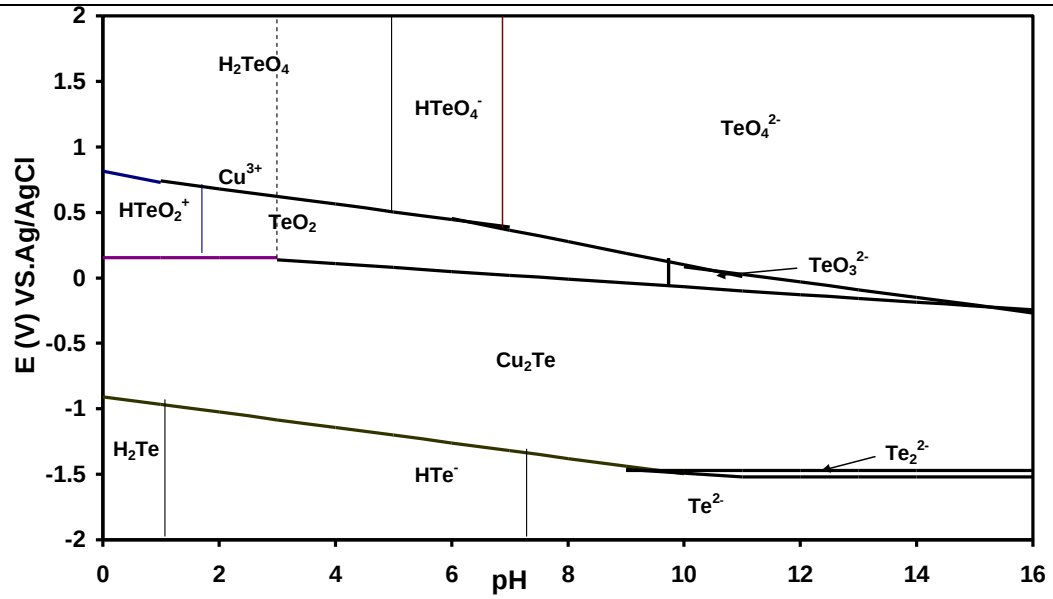

Figure 1: (a) pH-potential diagram of Cu-Te-H_2O system for a solution containing 1 mM $CuCl_2$ and 2 mM TeO_2 and 0.5 M citric acid. The potential was established with respect to Ag/AgCl reference electrode at room temperature. The relevant equilibrium reactions for plotting this diagram are listed in 5(a) Cu-Te-H_2O system.

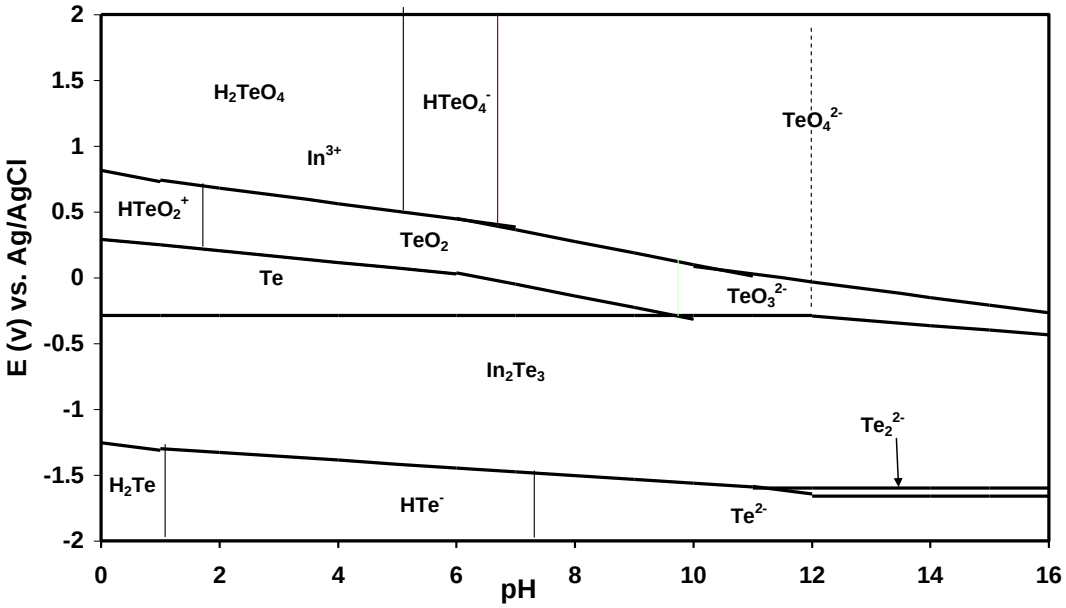

Figure 1: (b) pH-potential diagram of In-Te-H_2O system for a solution containing 10 mM $InCl_3$ and 2 mM TeO_2 and 0.5 M citric acid. The potential was established with respect to and Ag/AgCl reference electrode at room temperature. The relevant equilibrium reactions for plotting this diagram are listed in 5(b) In-Te-H_2O system.

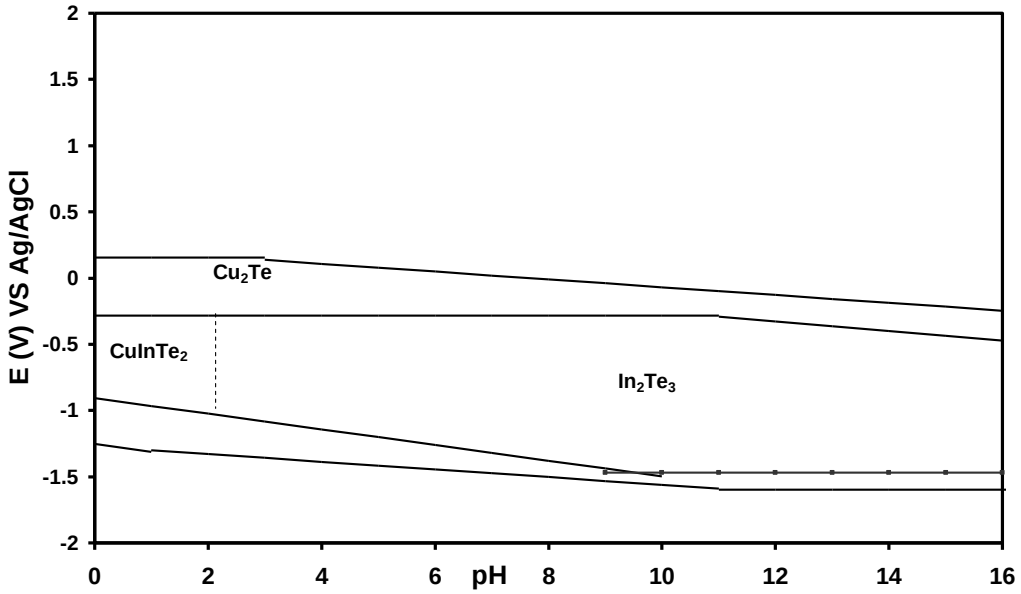

Figure 1(c) overlapped pH-potential diagram for Cu-Te-H_2O and In-Te-H_2O systems.

2. Linear Sweep Voltametry of $CuInTe_2$

LSV was recorded at room temperature for an unstirred solution containing Cu^{2+}, In^{+3}, and $HTeO_2^+$ solution and is shown in Figure 2. The cathode peak (A) at 190 mV vs Ag/AgCl can be attributed to the deposition of Cu_xTe because of the ease reduction of Te (E_o = +0.593 mV) and Cu (E_o = +0.521 mV) ions. As the formation of Cu_xTe is controlled by the diffusion of $HTeO_2$, the deposition current is independent of potential up to about 600 mV. The nucleation loop defines the onset of indium ion reduction (E_o = -0.338 mV) to deposit $CuInTe_2$ just above 600 mV vs Ag/AgCl. The deposition efficiency reaches its maximum at about 820 mV (B) where H_2 evolution and the formation of H_2Te begin.

The electro-deposition in this work was carried out under deposition potential in the range between 650 and 750 mV vs Ag/AgCl. During the reverse sweep in which the cathode voltage returns to 0 volts, the dissolution of $CuInTe_2$ and Cu_xTe phases are indicated by the peaks C and D, respectively, as shown in the voltammogram in Figure 2.

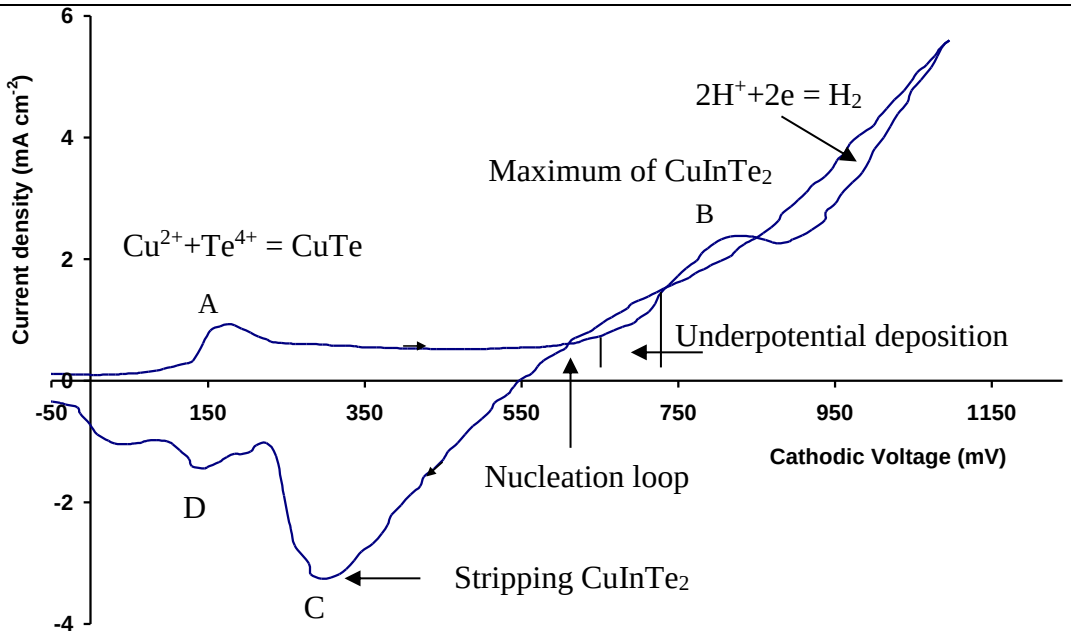

Figure 2: Voltammogram for $CuInTe_2$ at room temperature, without stirring the electrolyte containing 1 mM $CuSO_4$, 10 mM $In_2(SO_4)_3$, 2 mM TeO_2 and 0.5 M citric acid. The arrows indicate the direction of the potential sweep with a scan rate of 10 mV s^{-1}.

3. Electrochemical data used to plot pH-potential diagrams

a. Cu-Te-H_2O system

Formulae 3 - 13 show the relevant reactions used to plot the pH-potential diagram for the Cu-Te-H_2O system shown in Figure 1 (a) [4].

$$2Cu^{2+} + HTeO_2^+ + 3H^+ + 8e \rightarrow Cu_2Te + 2H_2O \quad (3)$$

$$2Cu^{2+} + Te + 4e \rightarrow Cu_2Te \quad (4)$$

$$2Cu^{2+} + TeO_2 + 4H^+ + 8e \rightarrow Cu_2Te + 2H_2O \quad (5)$$

$$Cu_2O + TeO_2 + 6H^+ + 6e \rightarrow Cu_2Te + 3H_2O \quad (6)$$

$$Cu_2O + Te + 2H^+ + 2e \rightarrow Cu_2Te + H_2O \quad (7)$$

$$Cu_2O + TeO_3^{2-} + 8H^+ + 6e \rightarrow Cu_2Te + 4H_2O \quad (8)$$

$$2Cu_2O + Te_2^{2-} + 4H^+ + 2e \rightarrow 2Cu_2Te + 2H_2O \quad (9)$$

$$Cu_2Te + 2H^+ + 2e \rightarrow H_2Te(g) + 2Cu \quad (10)$$

$$Cu_2Te + H^+ + 2e \rightarrow HTe^- + 2Cu \quad (11)$$

$$Cu_2Te + 2e \rightarrow Te^{2-} + 2Cu \quad (12)$$

$$2Cu_2Te + 2e \rightarrow Te_2^{2-} + 4Cu \quad (13)$$

b. In-Te-H_2O system

Formulae 14 - 23 show the relevant reactions used to plot the pH-potential diagram for the In-Te-H_2O system shown in Figure 1 (b) [4].

$$2In^{3+} + 3HTeO_2^+ + 9H^+ + 18e \rightarrow In_2Te_3 + 6H_2O \quad (14)$$

$$2In^{3+} + 3Te + 6e \rightarrow In_2Te_3 \quad (15)$$

$$2In^{3+} + 3TeO_2 + 12H^+ + 18e \rightarrow In_2Te_3 + 6H_2O \quad (16)$$

$$In_2O_3 + 3TeO_2 + 18H^+ + 18e \rightarrow In_2Te_3 + 9H_2O \quad (17)$$

$$In_2O_3 + 3TeO_3^{2-} + 24H^+ + 18e \rightarrow In_2Te_3 + 12H_2O \quad (18)$$

$$2In_2O_3 + 6Te + 12H^+ + 12e \rightarrow 2In_2Te_3 + 6H_2O \quad (18)$$

$$2In_2O_3 + 3Te_2^{2-} + 12H^+ + 6e \rightarrow 2In_2Te_3 + 6H_2O \quad (19)$$

$$In_2Te_3 + 6H^+ + 6e \rightarrow 3H_2Te(g) + 2In \quad (20)$$

$$In_2Te_3 + 3H^+ + 6e \rightarrow 3HTe^- + 2In \quad (21)$$

$$In_2Te_3 + 6e \rightarrow 3Te^{2-} + 2In \quad (22)$$

$$2In_2Te_3 + 6e \rightarrow 3Te_2^{2-} + 4In \quad (23)$$

4. Characterisation of $CuInTe_2$

a. X-ray diffraction

Figure 3(a) shows a typical XRD pattern obtained for as-deposited and heat treated layers. The as-deposited layers indicate the presence of three main peaks arising from reflections at (112), (204/220) and (116/312) atomic planes. After heat treatment of these layers at 400°C for 20 minutes in air atmosphere, the intensities of above three peaks increase with decreasing peak widths. The use of Scherrer equation , $l = \lambda / (\beta Cos\theta)$ Yield ~24 nm for the grain size (l) of $CuInTe_2$ present in these layers. In the above equation, λ is the wavelength of incident X-rays, β is the full width at half maximum and θ is the centre angle of the peak.

The heat treatment improves crystallization of the material. The formation of large grains by coalescing of smaller grains drastically reduce grain boundary scattering of charge carriers improving the electrical conduction. This process also makes the layers more uniform and eliminates many possible defects within the material layer.

Figure 3(b) shows XRD pattern of heat treated $CuInTe_2$ layers electrodeposited at four different cathode voltages. Each pattern contains strong peaks (112), (204), (312) and (400) indicating that the films are polycrystalline in nature, with a mainly tetragonal chalcopyrite structure. Te peaks are observed for growth at low voltages, which tend to disappear at higher cathode voltages due to incorporation of indium into the layers to form $CuInTe_2$. The appearance of peaks from $CuTe_2$ compounds at 600 mV vs Ag/AgCl suggests the thermodynamic ability of reaction 5 ahead of other possible reaction mechanisms. The presence of the four characteristic peaks (112), (204), (312) and (400) indicates that the main phase is $CuInTe_2$.

The observation of the three main peaks corresponding to $CuInTe_2$ confirms the feasibility of co-electro-deposition of this material from its pre-cursors. Comparison of these results with reports in the literature [5,6,7,8] also shows that electrochemical deposition is a suitable technique for the growth of thin films based on $CuInTe_2$ material with the required structural properties.

b. Optical absorption

The energy band gap of the material was estimated by measuring the optical absorption coefficient (α) as a function of wavelength and by plotting $(\alpha h\nu)^2$ versus the photon energy $(h\nu)$. Near the absorption edge, (α) is given by the equation

$$\alpha = \frac{k}{h\nu}\left(h\nu - E_g\right)^{\frac{n}{2}} \qquad (2)$$

where *k* is a constant, h is Planck's constant, E_g is energy band gap and ν is the frequency of light, and $n = 1$ for a direct band gap semiconductor. Assuming CIT films as single phase material (where $A \propto \alpha$), the equation can be re-arranged as shown by equation (3)

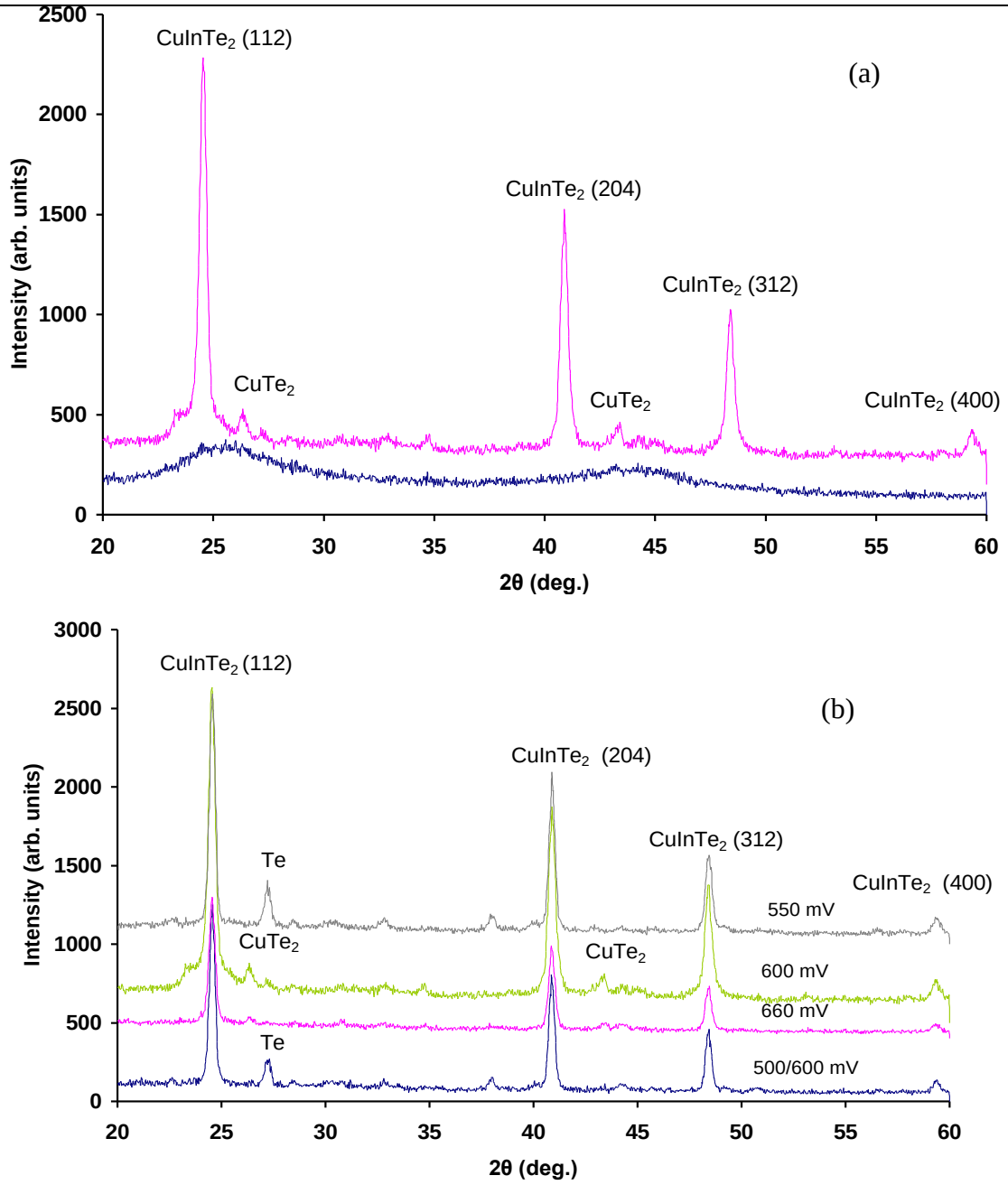

Figure 3: XRD pattern of (a) As-deposited and heat treated $CuInTe_2$ layers, and (b) heat treated $CuInTe_2$ layers electrodeposited at different cathode voltages.

$$(\alpha h\nu)^2 = k\left(h\nu - E_g\right) \qquad (3)$$

The band gap energy of the material was estimated by measuring the optical absorption as a function of the photon energy of light. Figure 4 show absorption spectra obtained for three layers grown at different voltages. The band gap energy of electro-

deposited layers varied in the range of 1.05–1.30 ± 0.02 eV. The reported band gap energies of stoichiometric $CuInTe_2$ at room temperature are 0.95 eV [9], Ishizaki et al. [6] reports 0.98 eV, while Marin et al. [10] reports 0.92–1.04 eV. Thus the higher band gap energy observed in this work indicates the inclusion of other phases, such as Cu_xTe and In_xTe, which have larger band gap energies than $CuInTe_2$. The vast difference in optical absorption suggests the non-uniformity in stoichiometry and the thickness of the materials layers. The slopes of these graphs provide indirect information of the material purity. The curves with high gradients indicate those of pure phases, while those with low gradients indicate mixed phases.

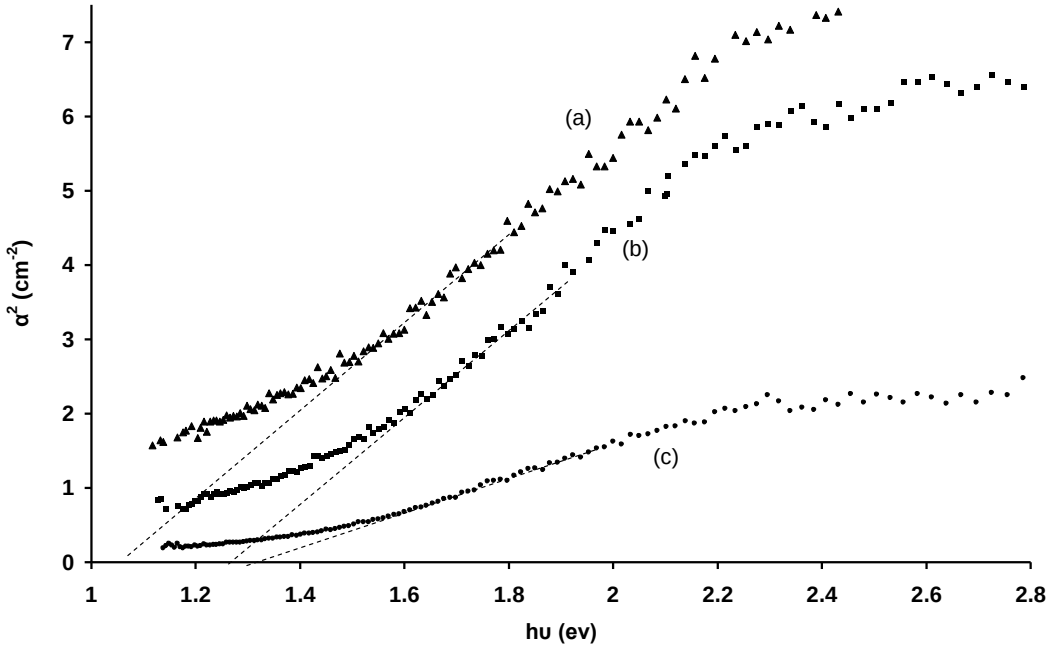

Figure 4: Optical absorption observed for $CuInTe_2$ layers grown by one step deposition at (a) 600 mV and two step deposition at (b) (550/660 mV vs Ag/AgCl) and (c) (550/600 mV vs Ag/AgCl).

c. Film thickness measurements

Figure 5 shows a typical scan from a Tallysurf for an electrodeposited $CuInTe_2$ layer across its edge. The thickness shown by the graph is ~1.2 µm, but it also shows the non uniformity of the thickness near the edge. The non-uniform thickness is expected at the edge of the sample due to the variation of the electrolyte level during electro-deposition. Uniform

thickness is usually observed away from the FTO/$CuInTe_2$ demarcation line. From a deposition current density of 1.4 mA cm^{-2} the theoretical thickness is estimated to be ~1.6 µm, suggesting about 75% Faradaic efficiency for deposition. The gravimetric measurements indicate a thickness of 1.6 µm for the sample.

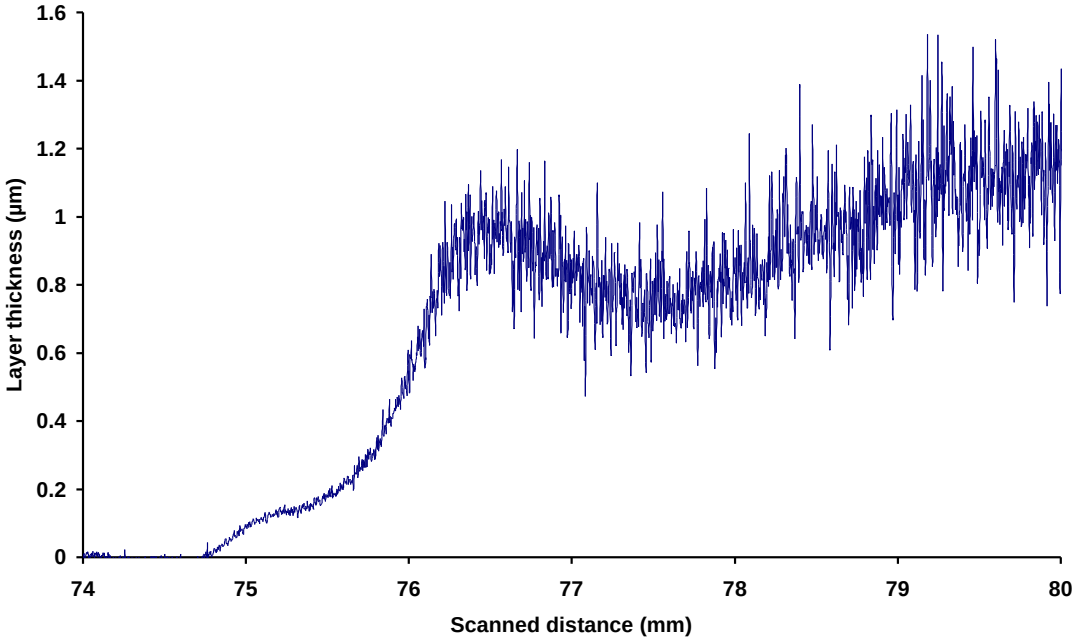

Figure 5: Tallysurf thickness profile of an electrodeposited $CuInTe_2$ layer.

5. Conclusion

This paper represents that $CuInTe_2$ layers can be deposited using electrochemical methods from aqueous solutions. The material produced during this preliminary study consists of traces of elemental tellurium, Cu_xTe and In_xTe. The material is polycrystalline, and XRD reveals a chalcopyrite structure very similar to that of $CuInSe_2$ materials. The band gap of these material layers varies in the range of 1.05–1.30 eV and is larger than the reported value of 0.95 eV for $CuInTe_2$. However, the morphology of layers and the doping levels need to be further improved.

References

1. T. Nakada, Y. Hirabayashi, T. Tokado, D. Ohmori, T. Mise, Sol. Energy 77, (2004) 739–747.
2. I. Repins, M. Contreras, M. Romero, Y. Yan, W. Metzger, J. Li, S. Johnston, B. Egaas, C. Dehart, J. Scharf, B. E. McCandless, R. Noufi, 33rd IEEE Photovoltaic Specialists Conference May 11-16th, 2008 San Diego California.
3. I. M. Dharmadasa, J. Haigh, J. Electrochem. Soc 153(1), (2006) G47–G52.
4. M. Pourbaix, Atlas of Electrochemical Equilibria in Aqueous Solution, Pregamon Press, Oxford, 1966, p.385.
5. C. D. Lokhande, S. H. Pawar, J. Phys. D. Appl. Phys. (Berl.) 20, (1987) 1213–1214.
6. T. Ishizaki, N. Saito, A. Fuwa, Surf. Coat. Tech. 182, (2004) 156–160.
7. A. Vijayakumar, T. Du, K. B. Sundaram, Appl. Surf. Sci. 242, (2005) 168–176.
8. J. L. Orts, R. Diaz, P. Herrasti, F. Rueda, E. Fatas, Sol. Energy Mater. Sol. Cells 91, (2007) 621–628.
9. David R. Lide, Handbook of chemistry & physics, 71st edn, (1990–1991), Table (12–59).
10. G. Marin, S.M. Wasim, G. Sanchez Perez, P. Bocaranda, A.E. Mora, J. Electron. Mater 27, (1998) 1351–1357.
11. A. M. Alshuaib, G. E. A. Muftah and E. M. Ashmila, "Morphology and composition of CulnSe2 that film deposited by Stacked Elemental Layers", Al-Tarbawi Journal, Al-Khoms. Libya, No. 9, July 2016, pp 462-475.

الفهـــــــــــرس